Clim. Past Discuss., https://doi.org/10.5194/cp-2018-175
Manuscript under review for journal Clim. Past
Discussion started: 17 December 2018

Climate of the Past Discussions

The relevance of mid-Holocene Arctic warming to the future

Masakazu Yoshimori[1,2] and Marina Suzuki[3]

[1]Faculty of Environmental Earth Science, Global Institution for Collaborative Research and Education, and Arctic Research Center, Hokkaido University, Sapporo, 060-0810, Japan
[2]Atmosphere and Ocean Research Institute, The University of Tokyo, Kashiwa, 277-8568, Japan
[3]Graduate School of Environmental Science, Hokkaido University, Sapporo, 060-0810, Japan

Correspondence to: Masakazu Yoshimori (masakazu@aori.u-tokyo.ac.jp)

Abstract. There remain substantial uncertainties in future projections of Arctic climate change. Schmidt et al. (2014) demonstrated the potential to constrain these uncertainties using a combination of paleoclimate simulations and proxy data. They found a weak correlation between sea ice changes in the mid-Holocene (MH) and in future projections, relative to the modern period. Such an "emergent constraint" provides a powerful tool to directly reduce the range of uncertainty, provided that the necessary paleoenvironmental information is available. In the current study, we examine the relevance of Arctic warming in the past to the future through process understanding, rather than seeking a statistical relation. We conducted a surface energy balance analysis on 10 atmosphere and ocean general circulation models under the MH and future RCP4.5-scenario forcing. We found that many of the dominant processes that amplify Arctic warming from late autumn to winter are common between the two periods, despite the difference in the source of the forcing (insolation vs. greenhouse gases). We also quantified the contribution of individual processes to the inter-model variance in the surface temperature changes. The controlling term varies with the season, but the results suggest that the models' representations of the surface albedo feedback, cloud greenhouse effect, turbulent surface heat fluxes, and indirect atmospheric stratification are important contributors. Based on the results for the Arctic warming mechanism obtained from this study, we conclude that proxy records of Arctic warming during the MH contain useful information that is relevant for understanding future Arctic climate change.

1 Introduction

The magnitude of climate change has been shown to be larger at high latitudes with paleoclimate evidence (Masson-Delmotte et al. 2013; Masson-Delmotte et al. 2006) and climate model equilibrium simulations (Manabe and Wetherald 1975; Stouffer and Manabe 1999). The Arctic is currently experiencing a more rapid warming than the rest of the world (Screen and Simmonds 2010; Serreze and Barry 2011), and this Arctic amplification is expected to continue at least until the end of this century (Collins et al. 2013; Laîné et al. 2016). A much slower rate of warming occurs in the Southern Ocean primarily due to oceanic processes (Armour et al. 2016) although it is possible that forcing and atmospheric processes also play a role (Marshall et al. 2014; Yoshimori et al. 2017). A substantial part of the uncertainty in the future Arctic warming projections is attributed to the differences among numerical models (Hodson et al. 2013). In addition, the projected range of

Clim. Past Discuss., https://doi.org/10.5194/cp-2018-175
Manuscript under review for journal Clim. Past
Discussion started: 17 December 2018

future Arctic warming within each scenario is much larger than that for the global mean. For example, the 90% confidence interval for the annual mean surface air temperature (SAT) change from the late 20th century to the late 21st century for the Arctic mean (67.5−90°N) is estimated as 1.6−6.9 °C while that for the global mean is 1.1−2.6 °C under the RCP4.5 scenario (Collins et al. 2013).

It is often assumed that the study of paleoclimate, particularly of warm periods, is useful for understanding future climate change projections. It is, however, nontrivial to demonstrate the relation between these two different time periods. Earlier studies discussed whether past climate can be used as an analogue for the future and discouraged general comparisons (Crowley 1990; Mitchell 1990). A relatively large number of studies have been conducted on the link between the past, including the last glacial maximum (LGM), and the future in the context of climate sensitivity based on processes and statistical correlation (Crucifix 2006; Hargreaves and Annan 2009; Hargreaves et al. 2007; Hargreaves et al. 2012; Yoshimori et al. 2009; Yoshimori et al. 2011). More recently, broader applications of the relation between paleo and future climate were summarized by Schmidt et al. (2014) who demonstrated the potential to constrain uncertainties using both paleoclimate simulations and proxy data. Indeed, they found a weak statistical inter-model correlation between the sea ice changes in the mid-Holocene (MH) and in future projections (RCP8.5 scenario) relative to the modern period. We note that Hargreaves and Annan (2009) also found statistically significant correlations between the mid to high northern latitude temperature for the MH and an elevated CO_2 scenario ($2\times CO_2$). The mechanism behind these emergent relations, however, remains unclear.

The purpose of the current study is to investigate commonalities and differences in the Arctic warming mechanisms in the past (MH) and future, and to discuss the relevance of Arctic warming in the MH for understanding future warming based on physical processes. We aim to obtain insight into the feasibility of constraining uncertainty in future climate change projections using paleoclimate data. The MH was chosen because proxy records suggest this period had a warmer Arctic state relative to the pre-industrial period, and multi-model simulations are already available from the Paleoclimate Modelling Intercomparison Project (PMIP3) and the Coupled Model Intercomparison Project (CMIP5). It should thus be straightforward to expand this approach to other time periods (e.g., the last interglacial, mid-Pliocene) once the multi-model simulations are easily accessible. The current study focuses on Arctic warming in general and not on the cause of sea ice reduction.

The data, models, and experiments are briefly explained in the next section. Analysis methods for diagnosing factors contributing to the surface temperature change in each model and to the inter-model differences are described in Sect. 3. Results are presented in Sect. 4, followed by discussion and conclusion in Sects. 5 and 6, respectively.

2 Climate models, experiments, and proxy data

The main analysis in the current study relies on the multi-model simulation data produced for the CMIP5 project (Taylor et al. 2012). The difference between the MH and preindustrial (PI) simulations (hereafter, ΔMH) and the difference between the RCP4.5 and historical (HIST) simulations (hereafter, ΔRCP4.5) are compared throughout the paper. The MH simulation

Clim. Past Discuss., https://doi.org/10.5194/cp-2018-175
Manuscript under review for journal Clim. Past
Discussion started: 17 December 2018

was designed and coordinated by the PMIP3 project (Braconnot et al. 2012). The MH aims to simulate the climate of 6000 years ago, and its forcing differs only in the earth's orbital configuration (obliquity, seasonal timing of precession, and eccentricity, Table 1) compared to the preindustrial simulations. For the MH and PI simulations, we use monthly climatological data averaged over periods longer than a century, which were archived as part of the CMIP5 dataset. The climatological data are constructed from monthly time series if these data are unavailable. The 20-year averages for 1980−1999 are used from the HIST simulations and those for 2080−2099 are used from the RCP4.5 simulations, so that ΔRCP4.5 represents the climate change for the entire 21st century, as in Laîné et al. (2016). We use 10 models that produced data for all four experiments (Table 2), and we analyze one simulation run for each model and each experiment. Prior to the analysis, all model output data are interpolated onto the T42 Gaussian grid (nominally 2.8°×2.8°) as in Laîné et al. (2016). A common land mask is constructed in such a way that a grid point is judged as ocean if more than 50% of models (that have fractional land cover data) indicate the grid point as ocean. The same procedure is used for the ocean mask, and consequently a small number of grid points are classified as neither ocean nor land.

The simulated ΔMH is compared with a temperature reconstruction based on proxy data. Sundqvist et al. (2010) compiled such a dataset primarily based on pollen and chironomids records. The oxygen isotope ratio from ice cores and borehole temperature are also used for the Greenland temperature. Another dataset is compiled by Bartlein et al. (2011) based on pollen records. We use the extended dataset of Bartlein et al. (2011) for the annual mean, which includes additional data from Schmittner et al. (2011) and Shakun et al. (2012) as in Harrison et al. (2014) and is available from the PMIP3 web site (https://pmip3.lsce.ipsl.fr/). The model ensemble mean data are further interpolated onto 2°×2° grids for comparison with Bartlein et al. (2011).

3 Analysis method

3.1 Surface energy balance and partial temperature changes

Processes contributing to the surface temperature difference between two experiments are evaluated based on the surface energy balance equation. The basic formulation follows Lu and Cai (2010). The surface energy balance equation for a reference climate is given by

$$(1-\alpha)S + F - R - H - L - Q = 0 \quad (1)$$

where $S = S^{clr} + S^{cld}$ and $F = F^{clr} + F^{cld}$ are the downwelling shortwave and longwave radiation at the surface, respectively, where the superscripts, "clr" and "cld", denote the clear-sky and cloud (total-sky – clear-sky) radiative effect, respectively. The upwelling longwave radiation is given by the Stefan-Boltzmann law, $R = \sigma T_s^4$, where σ is the Stefan-Boltzmann constant and the surface emissivity is assumed to be one. H and L are the sensible and latent heat fluxes, respectively, and Q represents the net surface energy flux including the latent heat consumed by snow/ice melting. In the ocean, Q is stored locally or transported. For the difference (Δ) between the two experiments, Eq. (1) becomes

Clim. Past Discuss., https://doi.org/10.5194/cp-2018-175
Manuscript under review for journal Clim. Past
Discussion started: 17 December 2018

Climate of the Past Discussions

$$4\sigma {T_s}^3 \Delta T_s = \begin{bmatrix} -\Delta\alpha S - \Delta\alpha\Delta S + (1-\Delta\alpha)S^{clr} + (1-\Delta\alpha)S^{cld} \\ +\Delta F^{clr} + \Delta F^{cld} - \Delta H - \Delta L - \Delta Q \end{bmatrix} \quad (2)$$

or more compactly

$$\Delta R = \sum_j \Delta R_j \quad (3)$$

where ΔR_j denotes the terms on the right side of Eq. (2).

The Stefan-Boltzmann law implies that a larger surface warming (ΔT_s) is required to balance the same amount of energy flux anomaly (ΔR) by emitting longwave radiation at a colder background temperature (T_s). Laîné et al. (2016) termed this effect the "surface warming sensitivity", whose importance for the Arctic amplification has been pointed out in multiple studies (Laîné et al. 2016; Laîné et al. 2009; Ohmura 1984, 2012; Pithan and Mauritsen 2014). The warming sensitivity and other energy flux terms may be converted to the same temperature scale (partial surface temperature changes)

$$\Delta T_s = \overline{\left(\frac{\partial T_s}{\partial R}\right)} \sum_j \Delta R_j{}' + \left(\frac{\partial T_s}{\partial R}\right)' \sum_j \overline{\Delta R_j} + \left(\frac{\partial T_s}{\partial R}\right)' \sum_j \Delta R_j{}' \quad (4)$$

where overbars and dashes represent the global mean and deviations from the global mean (local anomaly), respectively. Note that previous studies used the tropical mean in place of the global mean (Laîné et al. 2016; Pithan and Mauritsen 2014). The left side of Eq. (4) is the simulated surface temperature change. The first, second, and third terms on the right side of Eq. (4) represent local feedbacks evaluated with the global mean warming sensitivity, global mean feedbacks with the local warming sensitivity, and local feedbacks with the local warming sensitivity, respectively. In Sect. 3a, each component of the first term is evaluated separately, and the second and third terms are evaluated collectively as the "S-B" effect and "synergy" effect, respectively (Table 3). We use the average of T_s from the paired experiments (PI and MH, or HIST and RCP4.5) to calculate $\partial R / \partial T_s$. Although using the average of two experiments or a single experiment for this term has little impact on the results of the current study, we found that the average provided better agreement between the two sides of Eq. (4) for larger perturbations such as a quadrupling of the CO_2 experiment. The diagnosis is made for each grid point and each month. All models are used in this analysis.

3.2 Interpretation of surface temperature change at partially ice-covered ocean grid points

The surface temperature archived in the CMIP5 dataset (ts) represents the grid-mean "skin" temperature. At the fractionally ice-covered ocean grid points, this variable is a mixture of the sea surface temperature (SST) and ice surface temperature. We assume that the surface temperature is reconstructed by

$$T_s = (1-A)T_o + AT_i \quad (5)$$

where T_o and T_i are the SST and ice surface temperature, respectively, and A is the ice concentration. The factors contributing to the surface temperature difference for the paired experiments are then diagnosed by

$$\Delta T_s = (1-A)\Delta T_o + A\Delta T_i + (T_i - T_o)\Delta A. \quad (6)$$

The first and second terms on the right side represent the effect of SST and ice surface temperature changes, respectively. The last term on the right side represents the effect of the ice concentration change, which is weighted by the surface temperature difference between ice and water: the reduction of sea ice cover (ΔA<0) and the exposure of the warmer ocean

Clim. Past Discuss., https://doi.org/10.5194/cp-2018-175
Manuscript under review for journal Clim. Past
Discussion started: 17 December 2018

surface to the atmosphere ($T_i - T_o < 0$) lead to an increase in the grid-mean surface temperature (ΔT_s). In the current analysis, T_o, T_i, and A are obtained from the average of paired experiments. We use T_o in place of T_i for ice-free ocean grids. Only five models (bcc-csm-1, CCSM4, CNRM-CM5, IPSL-CM5A-LR, and MRI-CGCM3) are used for this analysis due to the availability of the required variables, and the consistency of the analysis is verified by agreement between the left and right sides of Eq. (6).

3.3 Factors responsible for the model spread

The fractional contribution of individual partial surface temperature changes (or feedbacks) to the inter-model spread of the simulated surface temperature change is given by

$$V_j = \sum_{k=1}^{n} \frac{(\Lambda_{j,k} - \overline{\Lambda}_j)(\Lambda_k - \overline{\Lambda})}{\sigma_\Lambda^2 (n-1)} \times 100\ [\%] \quad (7)$$

where V_j is the fractional contribution and Λ is the surface temperature change. The subscripts j and k denote indices for feedbacks (jth feedback) and models (kth model out of n models), respectively. The overbars denote the average over the feedbacks ($\overline{\Lambda}_j$), or over both the feedbacks and models ($\overline{\Lambda}$). σ_Λ is the inter-model standard deviation of the total (or simulated) surface temperature change. The numerator represents the product of the model spread for each feedback and the model spread for the total feedback while the denominator represents the ensemble variance of the total feedback. Here, the key points are: 1) V_j accounts for 100% of the surface temperature change when summed over the feedbacks; 2) positive V_j means that the jth feedback amplifies the model spread while negative V_j means that it suppresses the model spread. We note that the same formula was used in Yoshimori et al. (2011) and the references therein. The statistical significance of the fractional contribution is tested using the Monte-Carlo method by randomly shuffling the model index (k) 10^5 times. The null hypothesis is that the V_j neither amplify nor suppress the model spread. When the original V_j is outside the range of the 5−95th percentile of V_j resulting from the shuffling, it is considered significant. The diagnosis is made separately for ocean and land averages in the Arctic region (north of 60°N). All models are used for this analysis.

4 Results

4.1 Simulated surface air temperature response

Figure 1 shows the ensemble mean of the annual mean SAT response for ΔMH and ΔRCP4.5. In both cases, the warming in the polar regions is larger than for the rest of the world, particularly in the Arctic (see also Table 2). This feature reflects the so-called Arctic warming amplification in ΔRCP4.5. The warming at high latitudes and cooling at low latitudes in ΔMH are consistent with the annual mean insolation anomaly caused by the obliquity difference. From this figure it is unclear whether the Arctic warming in ΔMH is due to forcing and/or feedbacks.

Figures 2a and 2b show the seasonal progress of the effective radiative forcing (ERF) for ΔMH and ΔRCP4.5, respectively. The ERF is the top-of-the-atmosphere radiation change induced by the forcing constituents and is computed here using an

Clim. Past Discuss., https://doi.org/10.5194/cp-2018-175
Manuscript under review for journal Clim. Past
Discussion started: 17 December 2018

atmospheric GCM with a prescribed pre-industrial climatological SST and sea ice distribution. While this so-called Hansen-style method (Flato et al. 2013; Hansen et al. 2005) is one of the standard procedures for calculating future scenario forcing, e.g., ΔRCP4.5, it is uncommon in paleoclimate applications. With this method, the ERF includes both rapid stratospheric and tropospheric adjustments as well as the land surface response to the instantaneous radiative forcing. Although the land surface response should not be considered as the forcing, we present the ERF to facilitate a consistent comparison between different perturbation experiments. As a supplementary reference, another measure of radiative forcing evaluated by $\Delta S(1-\alpha)/4$ is presented for ΔMH in Fig. S1. Here, ΔS is the insolation anomaly and α is the pre-industrial planetary albedo. The ΔMH forcing patterns in both Fig. 2a and Fig. S1 are qualitatively similar to the familiar insolation anomaly ΔS (e.g., Fig. 1 in Ohgaito and Abe-Ouchi 2007): an increase and a decrease in summer and autumn, respectively, in the Northern Hemisphere, and an increase and a decrease in autumn and summer, respectively, in the Southern Hemisphere. The ΔRCP4.5 ERF is, in contrast, spatially and seasonally more homogeneous. Figures 2c and 2d show the ensemble mean of the seasonal progress of SAT changes for ΔMH and ΔRCP4.5, respectively. A common and striking feature is that the maximum Arctic warming occurs in autumn when the ERF is negative or weakly positive. This result suggests that feedbacks play an important role in shaping the seasonality of the Arctic warming for both ΔMH and ΔRCP4.5. This interpretation is in line with Zhang et al. (2010) for ΔMH and Laîné et al. (2016) for ΔRCP4.5.

Figure 3 shows SAT changes over the land and ocean for individual models. The seasonality of the SAT change over land is distinct between ΔMH and ΔRCP4.5, but there are some similarities over the ocean: the warming is modest in summer and largest in autumn. Significantly, the model spread over the ocean is also larger in autumn than in summer. The maximum land warming in summer for ΔMH corresponds to the maximum local insolation anomaly, and it thus may appear that the SAT warming over land is not related to the SAT warming over the ocean. However, there are strong cross-model correlations at the 5% statistical significance level (Student's *t*-test) between the land and ocean for the October-November-December (OND) mean as well as for the annual mean (Table 4). The statistically significant cross-model correlations at the 5% level also exist for ΔRCP4.5 (Table 4). In addition, the inter-model variance of the Arctic-mean SAT anomaly is larger over the ocean than over land. Although the available surface temperature proxy data for the mid-Holocene Arctic are more abundant on land than over the ocean (Bartlein et al. 2011; Sundqvist et al. 2010), it is useful to focus our analysis on the oceanic region, which has a larger response, and to explore which processes are responsible for the model difference there. We note that there is no statistically significant correlation at the 5% significance level between ΔMH and ΔRCP4.5 for either the OND or annual means (for both the Arctic ocean and land).

4.2 Comparison with proxy data

Figure 4 shows the ensemble mean of the simulated ΔMH annual mean, July, and January SAT anomalies superimposed with the reconstructed SAT anomaly at proxy sites taken from Sundqvist et al. (2010). We note that detailed comparison with earlier PMIP1 and PMIP2 simulations was given by Zhang et al. (2010). There is substantial disagreement between the model and the reconstruction: the simulated warming is, in general, underestimated in January as well as in the annual mean

Clim. Past Discuss., https://doi.org/10.5194/cp-2018-175
Manuscript under review for journal Clim. Past
Discussion started: 17 December 2018

by several degrees. Although better agreement is seen in July, the simulated warming is overestimated at some North American sites. O'Ishi and Abe-Ouchi (2011) reported that the model-data discrepancy improved substantially when the interaction between the MH climate change and vegetation distribution change is included in one model although the improvement is somewhat limited in other models (Zhang et al. 2010). Unfortunately, none of the models analyzed in the current study include this dynamic vegetation feedback. Comparisons of the model ensemble mean with Bartlein et al. (2011) for the ΔMH annual mean, warmest month, and coldest month are shown in Fig. S2. We note that more comprehensive comparison with PMIP2 and CMIP5 simulations was given by Harrison et al. (2014). Again, the model-data discrepancy is large although the qualitative tendencies of the warming in parts of Scandinavia appear in both. While these limitations need to be kept in mind, they do not reduce the significance of the following results on the understanding of the Arctic warming process.

4.3 Partial temperature change

Figure 5 shows the contribution of individual energy flux components to the surface temperature change (partial T_s changes) in the Arctic ocean diagnosed by the feedback analysis described in Sect. 3a. As expected, the simulated T_s changes (black lines) are reproduced by the sum of the individual contributions (blue dashed lines), indicating that the decomposition is useful.

For the case of ΔMH, the clear-sky shortwave radiation component (clr_sw) plays an important role, which is largely driven by the astronomical forcing and does not play a large role in ΔRCP4.5. The surface albedo feedback is distinctly positive from June to September for ΔMH and from April to September for ΔRCP4.5. The increased shortwave radiation reaching the sea surface through the albedo feedback is counteracted by the increased net surface heat flux term (surface), implying that the extra energy is likely stored in the form of ocean heat content. The net result is a small surface warming in summer. It is a common feature of both ΔMH and ΔRCP4.5 that the shortwave cloud radiative effect (cld_sw) weakens warming by the albedo feedback. This cancelling role of clouds in the warm season is consistent with previous studies using future climate projections (Crook et al. 2011; Laîné et al. 2016; Lu and Cai 2009).

From October to January for both ΔMH and ΔRCP4.5, the positive net surface heat flux term is counteracted by the negative surface turbulent flux terms (evap and sens), indicating that the heat is released from the ocean to the atmosphere in the form of latent and sensible heat fluxes. It is, however, unclear how the heat release to the atmosphere leads to the surface warming (or more precisely grid-mean skin temperature rise). This point is discussed in the next subsection in detail. It is a common feature of both ΔMH and ΔRCP4.5 that the longwave cloud radiative effect (cld_lw) helps warming by the net surface heat flux term. This amplifying role of clouds in the cold season is consistent with previous studies using future climate projections (Laîné et al. 2016; Yoshimori et al. 2014). The general increase of cloud cover in autumn to winter for both ΔMH and ΔRCP4.5 is consistent with the enhanced greenhouse effect of clouds (Fig. 6a and 6c).

Throughout the year, the clear-sky longwave radiation component (clr_lw) exhibits a large contribution and follows the shape of the seasonal progress of the total response. While this term includes the effect of the water vapor feedback (and also

Clim. Past Discuss., https://doi.org/10.5194/cp-2018-175
Manuscript under review for journal Clim. Past
Discussion started: 17 December 2018

the radiative forcing of greenhouse gases for the case of ΔRCP4.5), obtaining a physical interpretation of the role of the surface temperature change is difficult. The difficulty arises because the primary component of clear-sky LW radiation is emitted from the atmospheric layer near the surface (Ohmura 2001) where the temperature is tightly coupled with the surface, thus obscuring the causality. The positive local feedbacks in the cold season with a larger local warming sensitivity make the synergy term an important contributor to the total response for both ΔMH and ΔRCP4.5, as found by Laîné et al. (2016) in future climate projections. For completeness, the same analysis for the land surface temperature is shown in Fig. S3.

4.4 Interpretation of surface temperature change in partially ice-covered ocean grids

Figure 7 shows the surface temperature change (left side of Eq. (6), ΔT_s) and the individual contributions of surface conditions (the individual terms on the right side of Eq. (6)). The surface air temperature change (ΔT_{as}) is also plotted for reference. The seasonal progress of ΔT_s closely follows that of ΔT_{as}, suggesting the importance of understanding the grid-mean surface temperature change. The figure indicates that the large increase in grid-mean surface temperature during winter is largely due to the ice surface temperature increase when the SST anomaly decreases seasonally through the oceanic heat release after its peak value (Figs. 8a and 8c). The reduction of sea ice cover makes a substantial contribution to the grid-mean surface temperature increase during autumn. Its peak contribution does not, however, coincide with the timing of the maximum ice concentration anomaly (ΔA, Figs. 9a and 9c) as the effect is weighted by the surface temperature difference between the sea ice and ocean ($T_i - T_o$). The magnitude of the SST anomaly effect on the grid-mean surface temperature change is small as the SST change itself is small due to the large heat capacity of sea water. Therefore, the interpretation of the results of the feedback analysis is that the oceanic heat release in the cold season represented by the positive net surface heat flux term in Fig. 5 contributes to the surface air temperature rise and subsequent ice (and grid-mean) surface temperature rise.

4.5 Factors for the inter-model difference in surface temperature changes

Figure 10 shows the fractional contribution of the partial surface temperature changes to the model spread in the total surface temperature changes. The average is taken for the Arctic ocean areas, and positive or negative values indicate factors increasing or reducing the model differences, respectively. In both the annual mean and OND mean and for both ΔMH and ΔRCP4.5, the downwelling clear-sky longwave radiation (clr_lw) exhibits a large positive contribution. This is unsurprising because this radiative flux largely reflects the surface air temperature, which is thermally coupled with the surface temperature as stated in the previous section. This term, however, also includes the effect of water vapor and lapse-rate changes, whose contributions are not evaluated separately here. In the annual mean, the surface albedo feedback exhibits the second largest contribution to the model spread for both ΔMH and ΔRCP4.5, indicating that it is important to constrain the surface albedo feedback to reduce the model spread in both cases. The net surface flux term (surface) exhibits a positive contribution to the model spread in both the annual and OND means although it is negative in summer (June-July-August, not shown). As the oceanic heat content is reduced in OND through latent and sensible heat fluxes, it is understandable that

Clim. Past Discuss., https://doi.org/10.5194/cp-2018-175
Manuscript under review for journal Clim. Past
Discussion started: 17 December 2018

these two terms have opposite sign to the net surface flux term (similarly the albedo feedback and net surface flux term have opposite signs in summer). This result suggests the importance of the representation of the turbulent surface fluxes in models, and further, yet indirectly, the atmospheric stratification (or inversion). While OND albedo feedback shows only a small contribution to the OND model spread, this result does not mean that the summer albedo feedback is irrelevant to the OND model spread. The current analysis method does not reveal the link between the feedbacks and response across seasons. A numerical experiment is necessary to investigate such a link. Here we only point out that the model variances of the sea ice concentration change peak in September-October (Figs. 9b and 9d), and there is a large inter-model variability in the absorption and release of heat in summer and late autumn (Figs. 8b and 8d). It is important to point out that the longwave cloud feedback (cld_lw) contributes positively to the model spread in both seasons for both ΔMH and ΔRCP4.5 although the inter-model variability in cloud cover peaks in summer for ΔMH and late autumn for ΔRCP4.5 (Figs. 6b and 6d). It is also important to notice that the synergy term, which results from the interaction between individual feedbacks and the surface warming sensitivity, contributes positively to the model spread. As the surface warming sensitivity depends on the background temperature, this result suggests that the differences in the reference surface temperature, i.e., model bias, has the potential to reduce the simulated model response. In summary, attention needs to be paid to the models' representation of surface albedo, turbulent heat fluxes, clouds, and temperature bias to reduce the differences in models' response. For completeness, the same analysis for the land surface temperature is shown in Fig. S4.

5 Discussions

In the current study, the energy balance analysis is conducted for the surface level, and hence the effect of air temperature change and the associated downward longwave radiation in the Arctic region is not separated into local or remote origins. Therefore, the current study provides only a local feedback perspective with regard to the relevance of mid-Holocene Arctic warming to the future. As the change in orbital configurations redistributes the insolation latitudinally, a significant change in the meridional heat transport is expected. The change in the meridional heat transport by both the atmosphere and ocean in response to the wider variety of orbital configurations is worth further investigation in the future.

We note that the processes responsible for the ΔRCP4.5 Arctic warming amplification for CMIP5 models was investigated in detail in Laîné et al. (2016) with a larger sample size (32 instead of 10). Their result is summarized as follows. The extra solar radiation reaches the sea surface through the surface albedo feedback due to the sea ice decrease in summer, which was then absorbed by the ocean (and used partially for further melting of sea ice). The maximum reduction of sea ice cover occurs in September when the sea surface temperature anomaly is also largest. As the colder season approaches, the exposed warm open water without the insulating effect of sea ice releases heat vigorously to the colder atmosphere, including the extra heat that was stored during the summer. The warming is amplified in winter near the surface because of 1) the strong atmospheric stratification that confines the warming to near the surface, 2) the cloud-induced greenhouse effect, which does not invoke the sun-shade effect when there is little insolation, and 3) the larger temperature response required by the nonlinearity of the Stefan-Boltzmann law at colder temperatures to achieve energy balance. Although our analysis method

does not quantify the effect of atmospheric stratification, the ice surface temperature rise following the winter oceanic heat release suggests the importance of stratification and the current results for ΔMH and ΔRCP4.5 are consistent with the above summary.

There remain outstanding issues to be explored. O'Ishi and Abe-Ouchi (2011) showed that the vegetation change in response to climate change in both the mid-Holocene and elevated CO_2 experiments amplifies the Arctic warming. In particular, the expansion of boreal forest in place of tundra lowers the surface albedo through earlier snow melting and leads to the amplification of continental warming in spring and subsequent maritime warming in winter. None of the models analyzed in the current study include the effect of climate-vegetation interaction. Therefore, the conclusion of the current study needs to be verified by models with a dynamic vegetation component.

The current study focuses on the mid-Holocene partly because multi-model simulations for this period are easily accessible through the CMIP5-PMIM3 archive, and the compiled reconstruction dataset is available. There are, however, other periods that appear to exhibit larger Arctic warming such as the last interglacial (MIS5e), MIS11, and mid-Pliocene (Berger et al. 2016; Dutton et al. 2015; Lunt et al. 2013). These warm periods surely would be useful for expanding the analysis conducted in this study. While the energy balance feedback analysis has been applied to the MH, LGM, and mid-Pliocene (Braconnot and Kageyama 2015; Hill et al. 2014), which are very useful for understanding past climate change, a study focusing on the relevance to the future is encouraged. On the other hand, expanding the current study to cases with more general astronomical forcing (e.g., only considering the effect of the obliquity change or precession change), and to consider the implications for the mechanism for glacial-interglacial cycles (e.g., Abe-Ouchi et al. 2013) may also be valuable.

6 Conclusions

Although the insolation in the Arctic region decreases in autumn for the MH relative to the modern period, the largest Arctic warming occurs in autumn. Although the elevated CO_2 radiative forcing is rather uniform globally and seasonally, the largest Arctic warming also occurs almost in the same season as for the MH. Within the limited range of processes investigated, the current study suggests that the dominant processes causing Arctic warming in the MH and in the future are common: albedo feedback in summer, and the consequent heat release from the ocean to the atmosphere in the colder season when the stratification is strong, and an increased greenhouse effect from clouds during the season with least insolation. Those processes are also found to be primarily responsible for the model spread. If the Arctic warming in the MH is simulated accurately, the reliability of the model's representation of those processes would increase. Thus, the reliability of the future projections would also increase. From this study, we conclude that proxy records of the Arctic warming for the MH contain useful information relevant to future Arctic climate change. The current disparity between the model and proxy reconstructions is, therefore, of concern. The inclusion of dynamic vegetation feedback discussed in the previous section has a high priority.

The relation between past and future climate is not due to a common forcing to the climate system but due to the feedbacks inherent in the climate system. Therefore, more effort should be made in seeking possible analogues between

physical processes in the past and future climate, rather than in the past forcing. Our study supports the conclusion by Mitchell (1990) that it is a necessary condition for models to be able to reproduce the MH climate to produce reliable future projections, and we conclude that the evaluation of the models' parameterization is embedded in the model validation exercise using proxy data.

Author contribution

This study was developed based on parts of MS's bachelor and master theses at Hokkaido University. MY designed the analysis. MS conducted initial analysis which was completed by MY. MY prepared the manuscript with contributions from MS. Both authors contributed to the interpretation of the results.

Competing interests

The authors declare that they have no conflict of interest.

Acknowledgements

The method for diagnosing the surface temperature change described in Sect. 3b originates from discussions with Dr. Alexandra Laîné in previous works. This study also benefitted from discussions with Dr. Ayako Abe-Ouchi. We acknowledge the World Climate Research Programme's Working Group on Coupled Modelling, which is responsible for CMIP, and we thank the climate modeling groups (listed in Table 2 of this paper) for producing and making available their model output. For CMIP the U.S. Department of Energy's Program for Climate Model Diagnosis and Intercomparison provides coordinating support and led the development of the software infrastructure in partnership with the Global Organization for Earth System Science Portals. We thank PMIP for coordinating the experiment and preparing the dataset. We also thank the developers of the freely available software, NCO, CDO, and NCL. The calculation of the radiative forcing with MIROC4m-AGCM was carried out using the JAMSTEC Earth Simulator 3, and the support from the MIROC model development team is appreciated. This study was supported by JSPS KAKENHI Grant Number JP17H06104 and the Arctic Challenge for Sustainability (ArCS) project of MEXT.

References

Abe-Ouchi, A., F. Saito, K. Kawamura, M. E. Raymo, J. Okuno, K. Takahashi, and H. Blatter: Insolation-driven 100,000-year glacial cycles and hysteresis of ice-sheet volume. *Nature*, **500**, 190-194, 2013.

Armour, K. C., J. Marshall, J. R. Scott, A. Donohoe, and E. R. Newsom: Southern Ocean warming delayed by circumpolar upwelling and equatorward transport. *Nature Geoscience*, **9**, 549-555, 2016.

Bartlein, P. J., and Coauthors: Pollen-based continental climate reconstructions at 6 and 21 ka: a global synthesis. *Climate Dynamics*, **37**, 775-802, 2011.

Berger, A., and Coauthors: Interglacials of the last 800,000years. *Reviews of Geophysics*, **54**, 162-219, 2016.

Braconnot, P., and M. Kageyama: Shortwave forcing and feedbacks in Last Glacial Maximum and Mid-Holocene PMIP3 simulations. *Philosophical Transactions of the Royal Society a-Mathematical Physical and Engineering Sciences*, **373**, doi:10.1098/rsta.2014.0424, 2015.

Braconnot, P., and Coauthors: Evaluation of climate models using palaeoclimatic data. *Nature Climate Change*, **2**, 417-424, 2012.

Collins, M., and Coauthors: Long-term Climate Change: Projections, Commitments and Irreversibility. *Climate Change 2013: The Physical Science Basis. Contribution of Working Group I to the Fifth Assessment Report of the Intergovernmental Panel on Climate Change* T. F. Stocker, D. Qin, G.-K. Plattner, M. Tignor, S.K. Allen, J. Boschung, A. Nauels, Y. Xia, V. Bex and P.M. Midgley, Ed., Cambridge University Press, 1029-1136, 2013.

Crook, J. A., P. M. Forster, and N. Stuber: Spatial Patterns of Modeled Climate Feedback and Contributions to Temperature Response and Polar Amplification. *Journal of Climate*, **24**, 3575-3592, 2011.

Crowley, T. J.: Are There Any Satisfactory Geologic Analogs for a Future Greenhouse Warming. *Journal of Climate*, **3**, 1282-1292, 1990.

Crucifix, M.: Does the Last Glacial Maximum constrain climate sensitivity? *Geophysical Research Letters*, **33**, doi:10.1029/2006gl027137, 2006.

Dutton, A., and Coauthors: Sea-level rise due to polar ice-sheet mass loss during past warm periods. *Science*, **349**, doi:10.1126/science.aaa4019, 2015.

Flato, G., and Coauthors: Evaluation of Climate Models. *Climate Change 2013: The Physical Science Basis. Contribution of Working Group I to the Fifth Assessment Report of the Intergovernmental Panel on Climate Change*, T. F. Stocker, D. Qin, G.-K. Plattner, M. Tignor, S.K. Allen, J. Boschung, A. Nauels, Y. Xia, V. Bex and P.M. Midgley, Ed., Cambridge University Press, 741-866, 2013.

Hansen, J., and Coauthors: Efficacy of climate forcings. *Journal of Geophysical Research-Atmospheres*, **110**, D18104, doi:10.1029/2005jd005776, 2005.

Hargreaves, J. C., and J. D. Annan: On the importance of paleoclimate modelling for improving predictions of future climate change. *Climate of the Past*, **5**, 803-814, 2009.

Hargreaves, J. C., A. Abe-Ouchi, and J. D. Annan: Linking glacial and future climates through an ensemble of GCM simulations. *Climate of the Past*, **3**, 77-87, 2007.

Hargreaves, J. C., J. D. Annan, M. Yoshimori, and A. Abe-Ouchi: Can the Last Glacial Maximum constrain climate sensitivity? *Geophysical Research Letters*, **39**, doi:10.1029/2012gl053872, 2012.

Harrison, S. P., and Coauthors: Climate model benchmarking with glacial and mid-Holocene climates. *Climate Dynamics*, **43**, 671-688, 2014.

Hill, D. J., and Coauthors: Evaluating the dominant components of warming in Pliocene climate simulations. *Climate of the Past*, **10**, 79-90, 2014.

Hodson, D. L. R., S. P. E. Keeley, A. West, J. Ridley, E. Hawkins, and H. T. Hewitt: Identifying uncertainties in Arctic climate change projections. *Climate Dynamics*, **40**, 2849-2865, 2013.

Laîné, A., M. Yoshimori, and A. Abe-Ouchi: Surface Arctic amplification factors in CMIP5 models: land and oceanic surfaces, seasonality. *Journal of Climate*, **29**, 3297-3316, 2016.

Laîné, A., M. Kageyama, P. Braconnot, and R. Alkama: Impact of Greenhouse Gas Concentration Changes on Surface Energetics in IPSL-CM4: Regional Warming Patterns, Land–Sea Warming Ratios, and Glacial–Interglacial Differences. *Journal of Climate*, **22**, 4621-4635, 2009.

Lu, J. H., and M. Cai: Seasonality of polar surface warming amplification in climate simulations. *Geophysical Research Letters*, **36**, L16704, doi:10.1029/2009gl040133, 2009.

——: Quantifying contributions to polar warming amplification in an idealized coupled general circulation model. *Climate Dynamics*, **34**, 669-687, 2010.

Lunt, D. J., and Coauthors: A multi-model assessment of last interglacial temperatures. *Climate of the Past*, **9**, 699-717.

Manabe, S., and R. T. Wetherald, 1975: Effects of Doubling CO_2 Concentration on Climate of a General Circulation Model. *Journal of the Atmospheric Sciences*, **32**, 3-15, 2013.

Marshall, J., and Coauthors: The ocean's role in polar climate change: asymmetric Arctic and Antarctic responses to greenhouse gas and ozone forcing. *Philosophical Transactions of the Royal Society a-Mathematical Physical and Engineering Sciences*, **372**, doi:10.1098/rsta.2013.0040, 2014.

Masson-Delmotte, V., and Coauthors: Information from Paleoclimate Archives. *Climate Change 2013: The Physical Science Basis.*, T. F. Stocker, D. Qin, G.-K. Plattner, M. Tignor, S.K. Allen, J. Boschung, A. Nauels, Y. Xia, V. Bex and P.M. Midgley, Ed., Cambridge University Press, 383-464, 2013.

Masson-Delmotte, V., and Coauthors: Past and future polar amplification of climate change: climate model intercomparisons and ice-core constraints. *Climate Dynamics*, **26**, 513-529, 2006.

Mitchell, J. F. B.: Greenhouse Warming - Is the Midholocene a Good Analog. *Journal of Climate*, **3**, 1177-1192, 1990.

O'Ishi, R., and A. Abe-Ouchi: Polar amplification in the mid-Holocene derived from dynamical vegetation change with a GCM. *Geophysical Research Letters*, **38**, doi:10.1029/2011gl048001, 2011.

Ohgaito, R., and A. Abe-Ouchi: The role of ocean thermodynamics and dynamics in Asian summer monsoon changes during the mid-Holocene. *Climate Dynamics*, **29**, 39-50, 2007.

Ohmura, A.: On the Cause of Fram Type Seasonal Change in Diurnal Amplitude of Air-Temperature in Polar-Regions. *J Climatol*, **4**, 325-338, 1984.

——: Physical basis for the temperature-based melt-index method. *Journal of Applied Meteorology*, **40**, 753-761, 2001.

——: Enhanced temperature variability in high-altitude climate change. *Theoretical and Applied Climatology*, **110**, 499-508, 2012.

Pithan, F., and T. Mauritsen: Arctic amplification dominated by temperature feedbacks in contemporary climate models. *Nature Geoscience*, **7**, 181-184, 2014.

Schmidt, G. A., and Coauthors: Using palaeo-climate comparisons to constrain future projections in CMIP5. *Climate of the Past*, **10**, 221-250, 2014.

Schmittner, A., and Coauthors: Climate sensitivity estimated from temperature reconstructions of the Last Glacial Maximum. *Science*, **334**, 1385-1388, 2011.

Screen, J. A., and I. Simmonds: The central role of diminishing sea ice in recent Arctic temperature amplification. *Nature*, **464**, 1334-1337, 2010.

Serreze, M. C., and R. G. Barry: Processes and impacts of Arctic amplification: A research synthesis. *Global and Planetary Change*, **77**, 85-96, 2011.

Shakun, J. D., and Coauthors: Global warming preceded by increasing carbon dioxide concentrations during the last deglaciation. *Nature*, **484**, 49-54, 2012.

Stouffer, R. J., and S. Manabe: Response of a coupled ocean-atmosphere model to increasing atmospheric carbon dioxide: Sensitivity to the rate of increase. *Journal of Climate*, **12**, 2224-2237, 1999.

Sundqvist, H. S., Q. Zhang, A. Moberg, K. Holmgren, H. Kornich, J. Nilsson, and G. Brattstrom: Climate change between the mid and late Holocene in northern high latitudes - Part 1: Survey of temperature and precipitation proxy data. *Climate of the Past*, **6**, 591-608, 2010.

Taylor, K. E., R. J. Stouffer, and G. A. Meehl: An Overview of Cmip5 and the Experiment Design. *Bulletin of the American Meteorological Society*, **93**, 485-498, 2012.

Yoshimori, M., T. Yokohata, and A. Abe-Ouchi: A Comparison of Climate Feedback Strength between CO2 Doubling and LGM Experiments. *Journal of Climate*, **22**, 3374-3395, 2009.

Yoshimori, M., A. Abe-Ouchi, and A. Laîné: The role of atmospheric heat transport and regional feedbacks in the Arctic warming at equilibrium. *Climate Dynamics*, **49**, 3457-3472, 2017.

Yoshimori, M., J. C. Hargreaves, J. D. Annan, T. Yokohata, and A. Abe-Ouchi: Dependency of Feedbacks on Forcing and Climate State in Physics Parameter Ensembles. *Journal of Climate*, **24**, 6440-6455, 2011.

Yoshimori, M., A. Abe-Ouchi, M. Watanabe, A. Oka, and T. Ogura: Robust Seasonality of Arctic Warming Processes in Two Different Versions of the MIROC GCM. *Journal of Climate*, **27**, 6358-6375, 2014.

Yoshimori, M., A. Abe-Ouchi, H. Tatebe, T. Nozawa, and A. Oka: The Importance of Ocean Dynamical Feedback for Understanding the Impact of Mid-High-Latitude Warming on Tropical Precipitation Change. *Journal of Climate*, **31**, 2417-2434, 2018.

Zhang, Q., H. S. Sundqvist, A. Moberg, H. Kornich, J. Nilsson, and K. Holmgren: Climate change between the mid and late Holocene in northern high latitudes - Part 2: Model-data comparisons. *Climate of the Past*, **6**, 609-626, 2010.

Clim. Past Discuss., https://doi.org/10.5194/cp-2018-175
Manuscript under review for journal Clim. Past
Discussion started: 17 December 2018

Climate of the Past Discussions
Open Access
EGU

Table 1 Orbital configurations for the PI and MH experiments from the PMIP3 web site. Parameters for PI may vary slightly with the model. The PI values here represent the values for the year 1850.

	Eccentricity	Obliquity (°)	Longitude of perihelion from the vernal equinox – 180 (°)
PI	0.016764	23.459	100.33
MH	0.018682	24.105	0.87

Clim. Past Discuss., https://doi.org/10.5194/cp-2018-175
Manuscript under review for journal Clim. Past
Discussion started: 17 December 2018

Climate of the Past Discussions
Open Access
EGU

Table 2 Models used in the current study and the annual, global and Arctic (north of 60°N) mean surface air temperature changes (°C).

Model	ΔMH		ΔRCP4.5	
	Global	Arctic	global	Arctic
bcc-csm1-1	-0.13	0.87	1.74	4.27
CCSM4	-0.22	0.01	1.83	3.89
CNRM-CM5	0.18	1.42	2.07	5.02
CSIRO-Mk3-6-0	0.02	0.43	2.37	3.06
FGOALS-g2	-0.75	-0.48	1.43	3.57
FGOALS-s2	-0.16	0.46	1.66	2.34
GISS-E2-R	-0.10	0.77	1.34	2.45
IPSL-CM5A-LR	-0.13	0.25	2.37	4.84
MIROC-ESM	-0.25	-0.27	2.58	6.00
MRI-CGCM3	-0.02	0.81	1.70	3.84
Mean	-0.16	0.43	1.91	3.93

Clim. Past Discuss., https://doi.org/10.5194/cp-2018-175
Manuscript under review for journal Clim. Past
Discussion started: 17 December 2018

Climate of the Past Discussions

Table 3 A list of the energy flux terms used in Figs. 5 and 10. Row #1 represents the strength of the global mean feedback calculated with local warming sensitivity. Rows #2−10 represent the strength of local feedback calculated with global mean warming sensitivity.

#	Symbol	Definition
1	S-B	nonlinearity of Stefan-Boltzmann law
2	alb	surface albedo change
3	alb*clr_sw	nonlinear effect of surface albedo and clear-sky shortwave radiation changes
4	clr_sw	clear-sky shortwave radiation change
5	clr_lw	clear-sky longwave radiation change
6	cld_sw	shortwave cloud radiative effect
7	cld_lw	longwave cloud radiative effect
8	evap	surface evaporation
9	sens	surface sensible heat flux
10	surface	net surface energy flux including latent heat for snow/ice melting and heat exchange with the subsurface
11	synergy	synergy term for local feedbacks and local warming sensitivity

5

Clim. Past Discuss., https://doi.org/10.5194/cp-2018-175
Manuscript under review for journal Clim. Past
Discussion started: 17 December 2018

Climate of the Past Discussions

Table 4 Correlation coefficients between the surface air temperature changes in the Arctic region (north of 60°N). ANN and OND stand for the annual mean and October-November-December mean, respectively. All numbers are statistically significant at the 5% level with the Student's *t*-test.

	ΔMH land (ANN; OND)	ΔRCP4.5 land (ANN; OND)
ΔMH ocean (ANN; OND)	0.94; 0.95	
ΔRCP4.5 ocean (ANN; OND)		0.89; 0.92

5

Clim. Past Discuss., https://doi.org/10.5194/cp-2018-175
Manuscript under review for journal Clim. Past
Discussion started: 17 December 2018

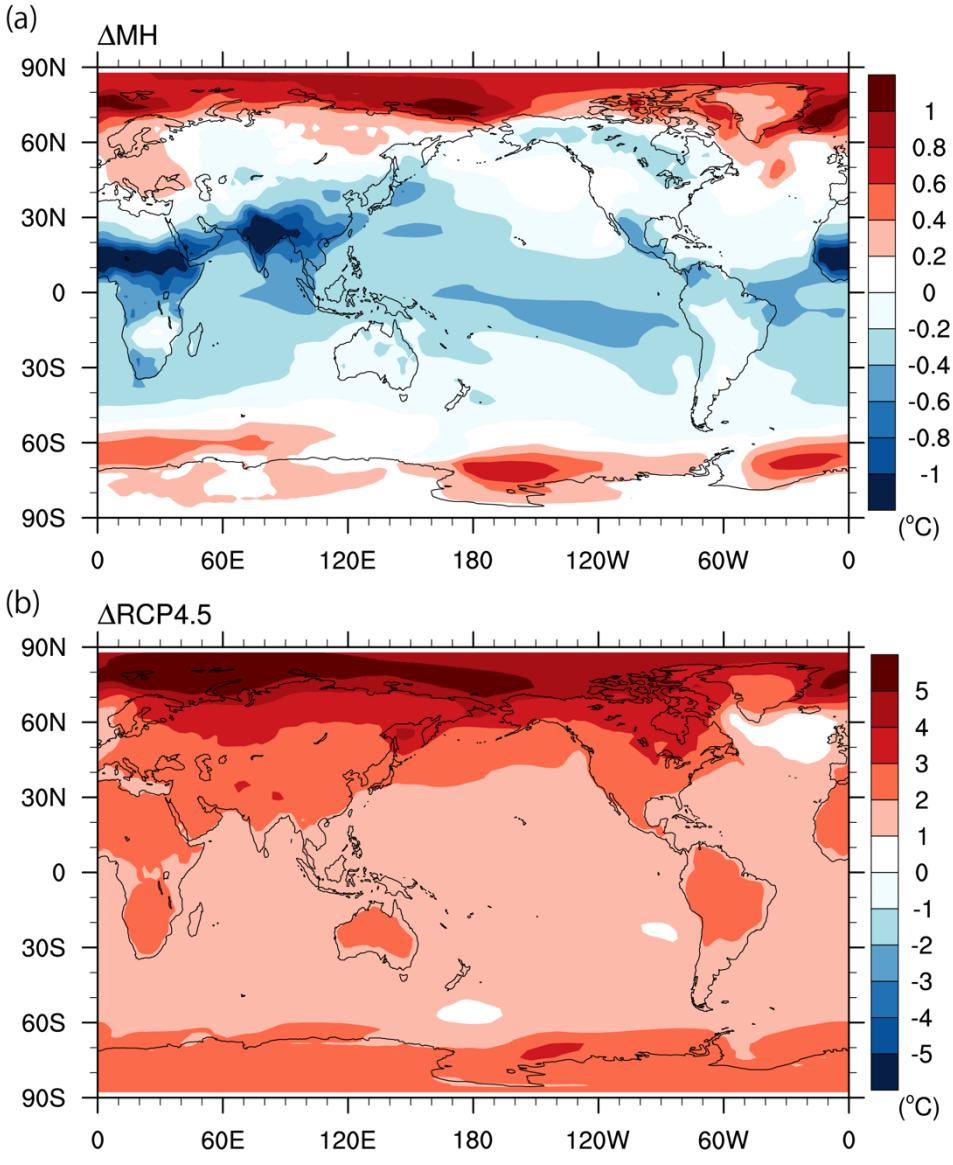

Figure 1 Multi-model mean (10 models) annual mean surface air temperature response (°C): (a) ΔMH; and (b) ΔRCP4.5.

Clim. Past Discuss., https://doi.org/10.5194/cp-2018-175
Manuscript under review for journal Clim. Past
Discussion started: 17 December 2018

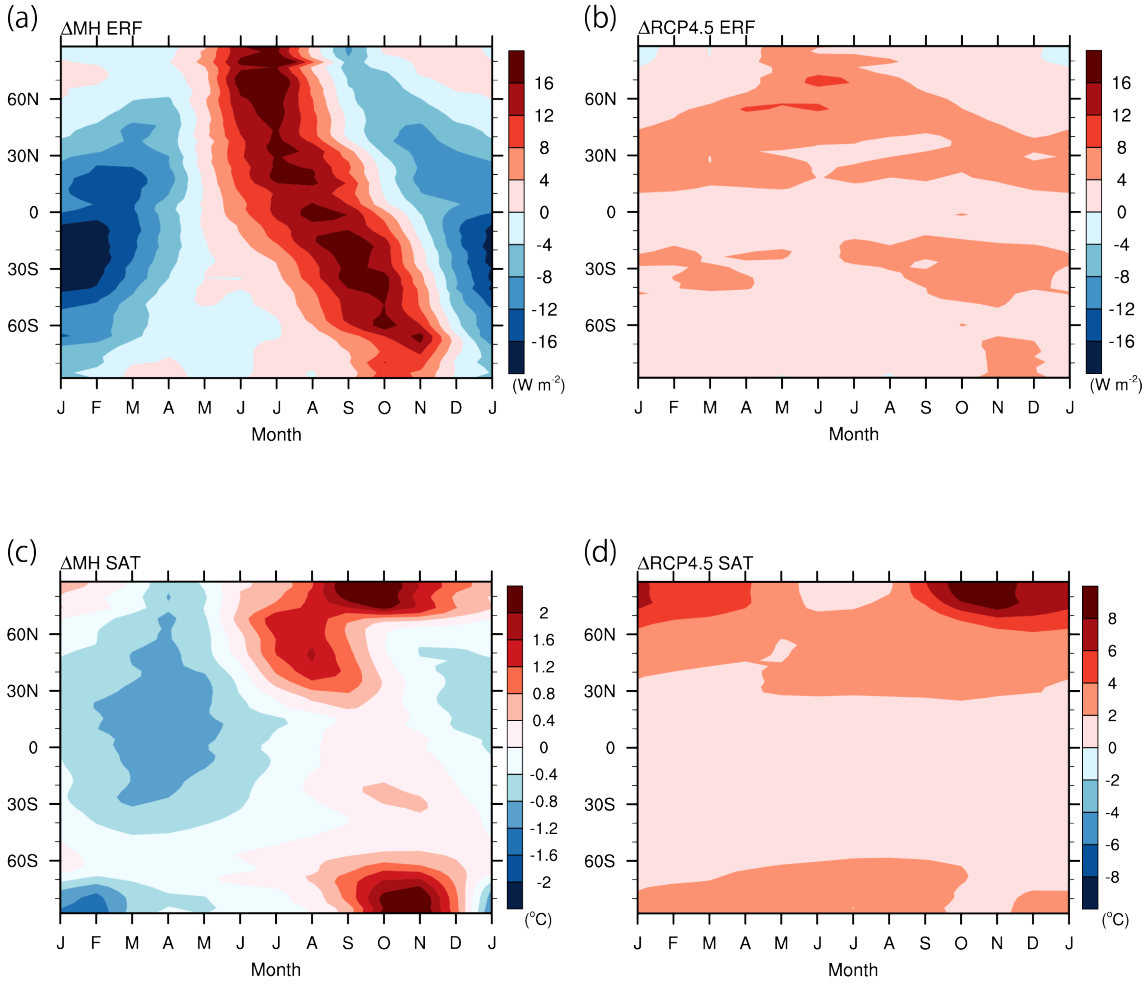

Figure 2 Seasonal progress of the zonal mean effective radiative forcing, ERF (top, W m^{-2}) and surface air temperature change (bottom, °C): (a) & (c) ΔMH; and (b) & (d) ΔRCP4.5. The ERF for ΔRCP4.5 is drawn using the data from Yoshimori et al. (2018), and it is computed in the current study for ΔMH. Both ERFs are constructed with a single model, MIROC4m-AGCM (Yoshimori et al., 2018). The surface air temperature changes are the means of all 10 models.

Clim. Past Discuss., https://doi.org/10.5194/cp-2018-175
Manuscript under review for journal Clim. Past
Discussion started: 17 December 2018

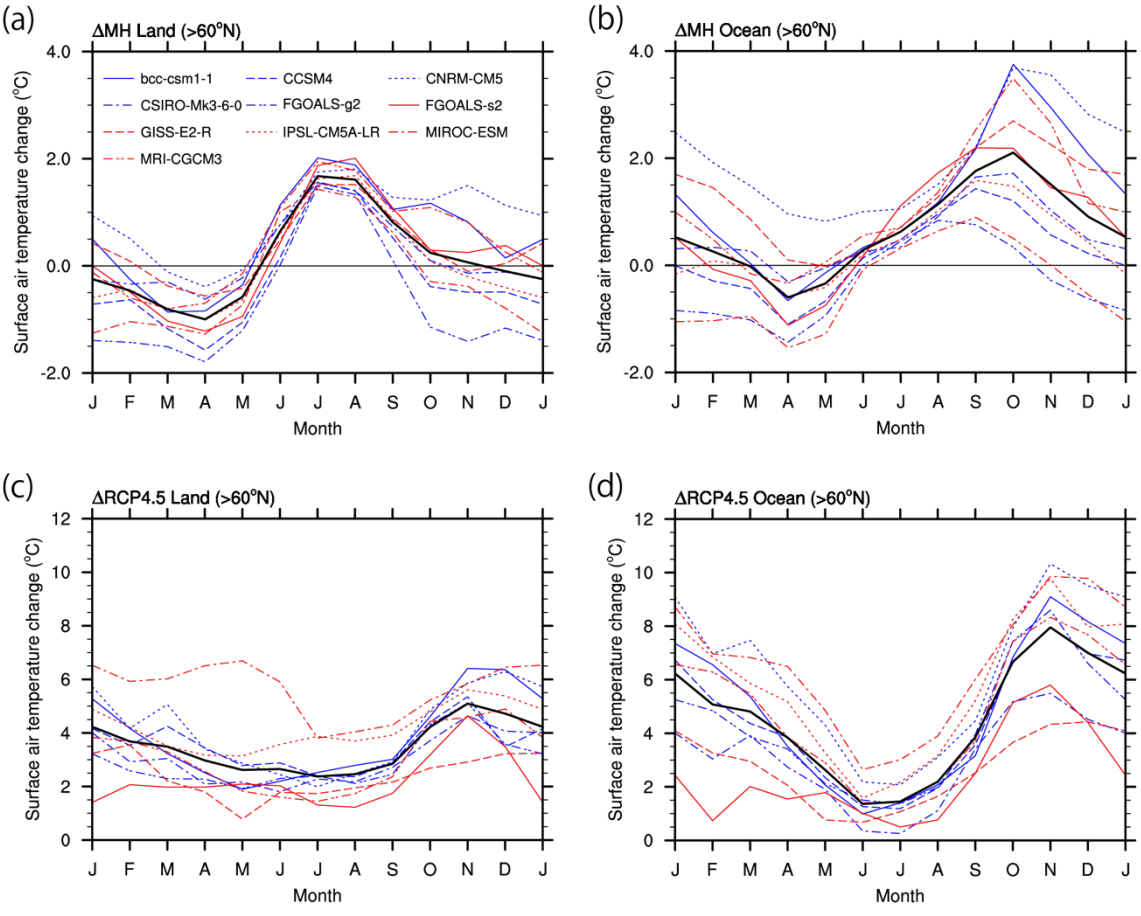

Figure 3 Seasonal progress of the surface air temperature change (°C) in the Arctic (north of 60°N): (a) ΔMH land; (b) ΔMH ocean; (c) ΔRCP4.5 land; and (d) ΔRCP4.5 ocean. Thick black lines show the multi-model mean.

Clim. Past Discuss., https://doi.org/10.5194/cp-2018-175
Manuscript under review for journal Clim. Past
Discussion started: 17 December 2018

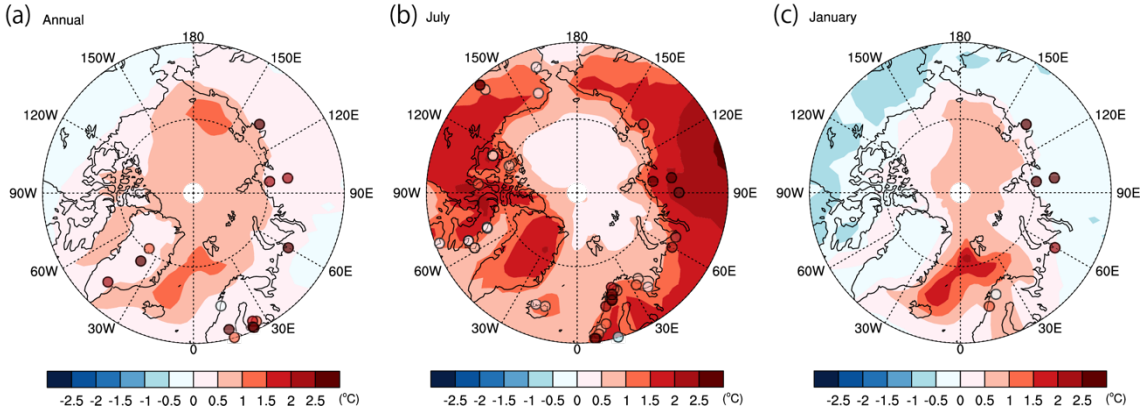

Figure 4 Surface air temperature anomaly (°C) for ΔMH from the simulations (shading) and reconstruction (solid circles): (a) annual mean; (b) July; and (c) January. The reconstruction data are taken from Sundqvist et al. (2010). The mean of all 10 model simulations was used.

Clim. Past Discuss., https://doi.org/10.5194/cp-2018-175
Manuscript under review for journal Clim. Past
Discussion started: 17 December 2018

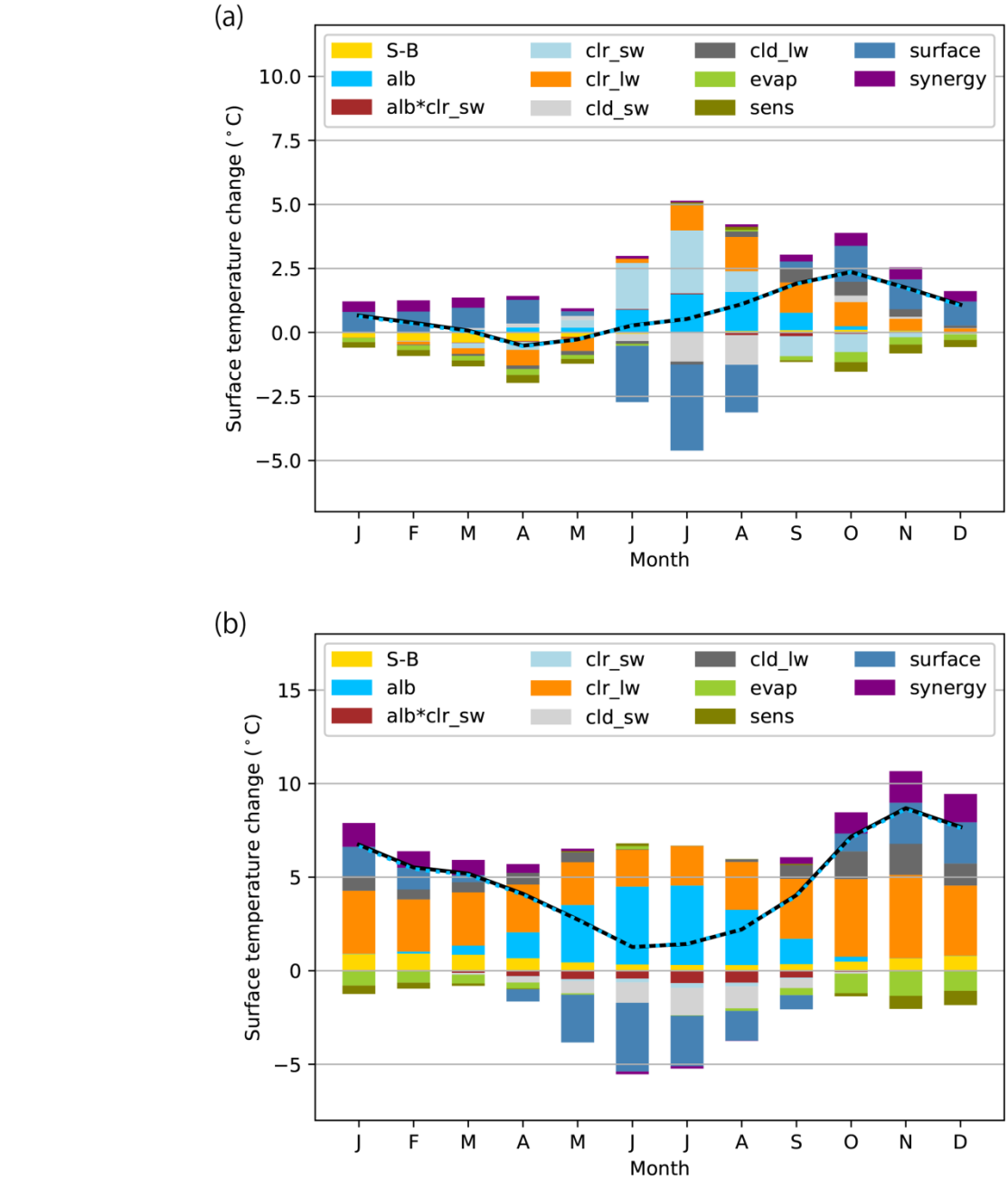

Figure 5 Simulated and diagnosed surface temperature changes (°C) for the ocean (north of 60°N): (a) ΔMH; and (b) ΔRCP4.5. The black lines denote simulated changes and blue dashed lines denote the sum of the diagnosed partial changes. The graphs represent the means of all 10 models. See Table 3 for the interpretation of each component.

Clim. Past Discuss., https://doi.org/10.5194/cp-2018-175
Manuscript under review for journal Clim. Past
Discussion started: 17 December 2018

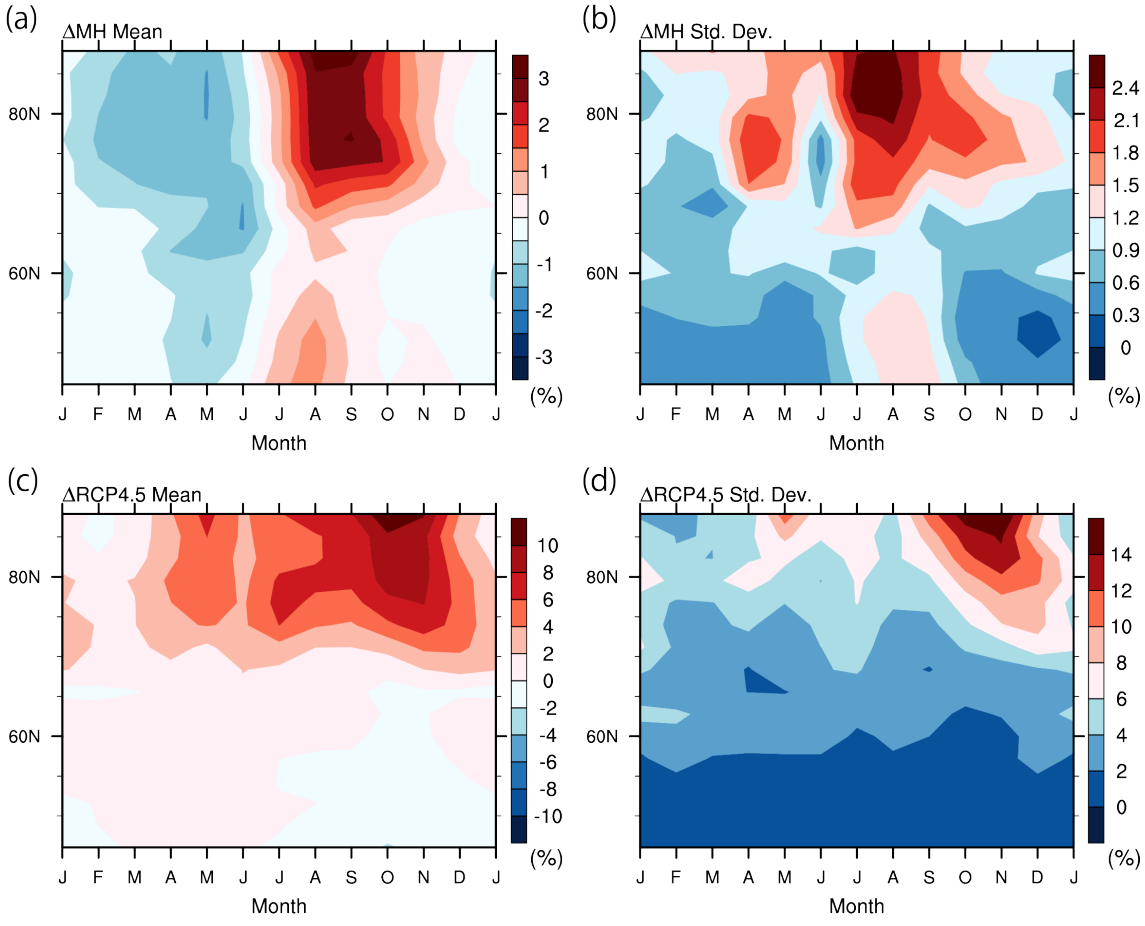

Figure 6 Seasonal progress of the total cloud fraction change (%) over the ocean (north of 60°N): (a) ΔMH ensemble mean; (b) ΔMH ensemble standard deviation; (c) ΔRCP4.5 ensemble mean; and (d) ΔRCP4.5 ensemble standard deviation. All 10 models are used.

Clim. Past Discuss., https://doi.org/10.5194/cp-2018-175
Manuscript under review for journal Clim. Past
Discussion started: 17 December 2018

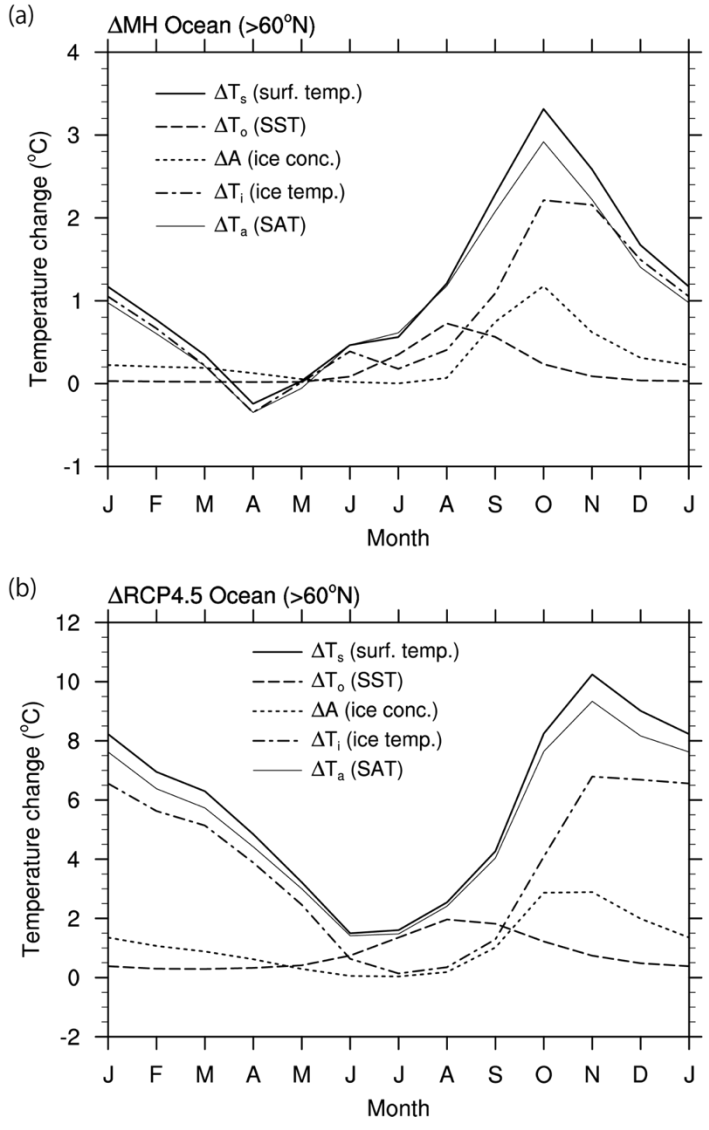

Figure 7 Contribution of the individual components to the surface temperature change (°C) over the ocean (north of 60°N): (a) ΔMH; and (b) ΔRCP4.5. The surface temperature change (ΔT_s) is decomposed into the components of the SST change (ΔT_o), sea ice concentration change (ΔA), and sea ice surface temperature change (ΔT_i). Simulated surface temperature and surface air temperature changes (ΔT_a) are also plotted for reference. Only 5 models are used.

Clim. Past Discuss., https://doi.org/10.5194/cp-2018-175
Manuscript under review for journal Clim. Past
Discussion started: 17 December 2018

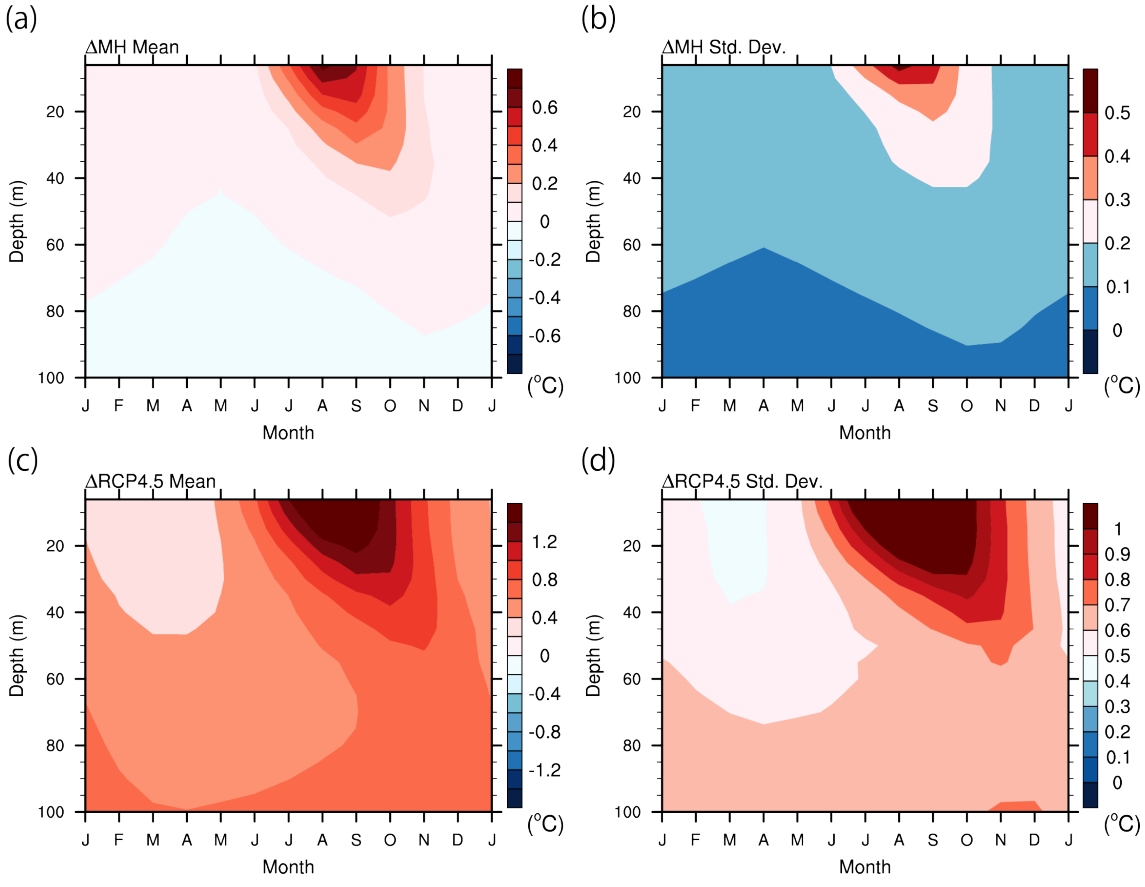

Figure 8 Same as in Fig. 6 but for the upper ocean temperature change (°C) (north of 60°N). Only 8 models are used (data from FGOALS-g2 and IPSL-CM5A-LR are unavailable).

Clim. Past Discuss., https://doi.org/10.5194/cp-2018-175
Manuscript under review for journal Clim. Past
Discussion started: 17 December 2018

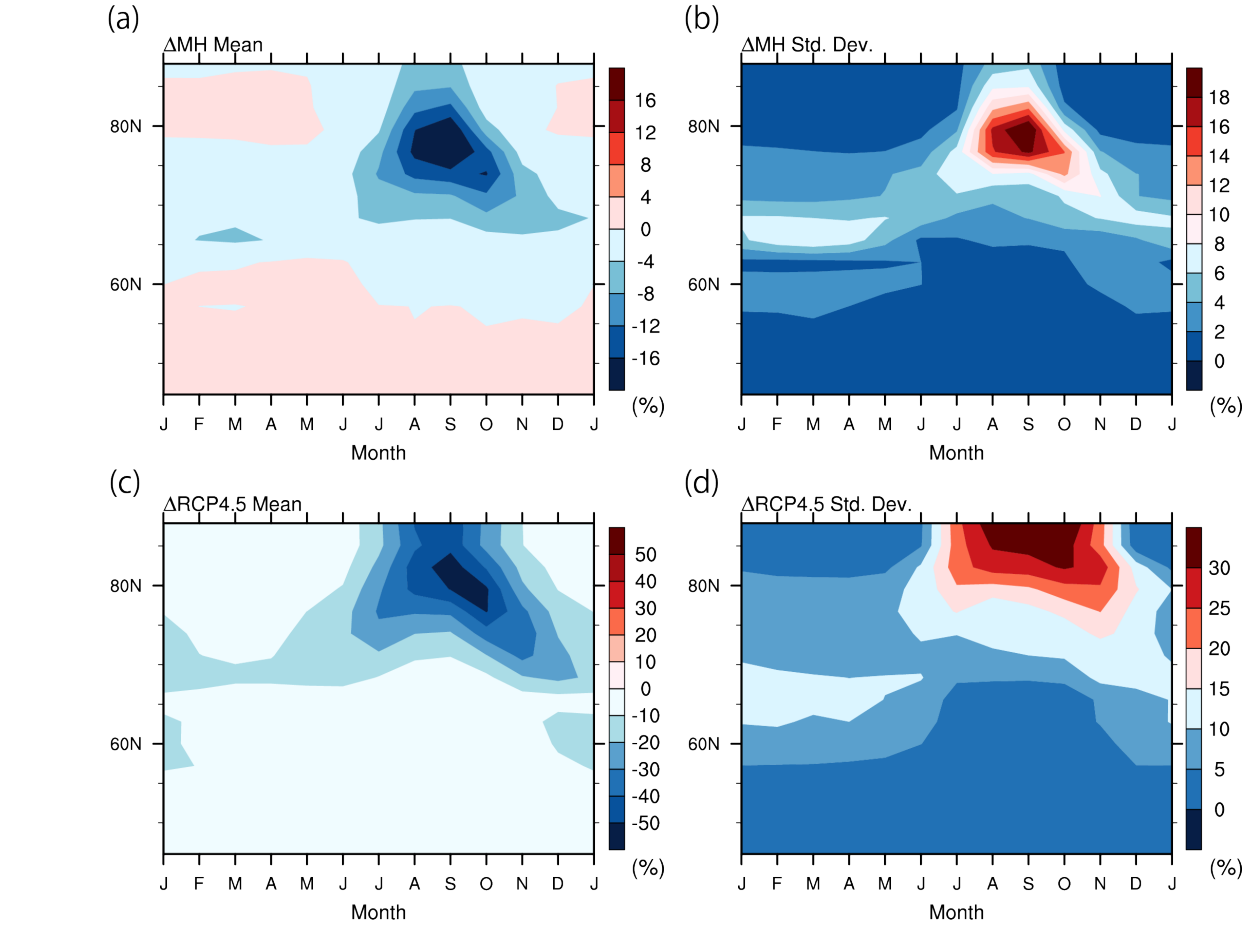

Figure 9 Same as in Fig. 6 but for the sea ice concentration (%) (north of 60°N). All 10 models are used.

Clim. Past Discuss., https://doi.org/10.5194/cp-2018-175
Manuscript under review for journal Clim. Past
Discussion started: 17 December 2018

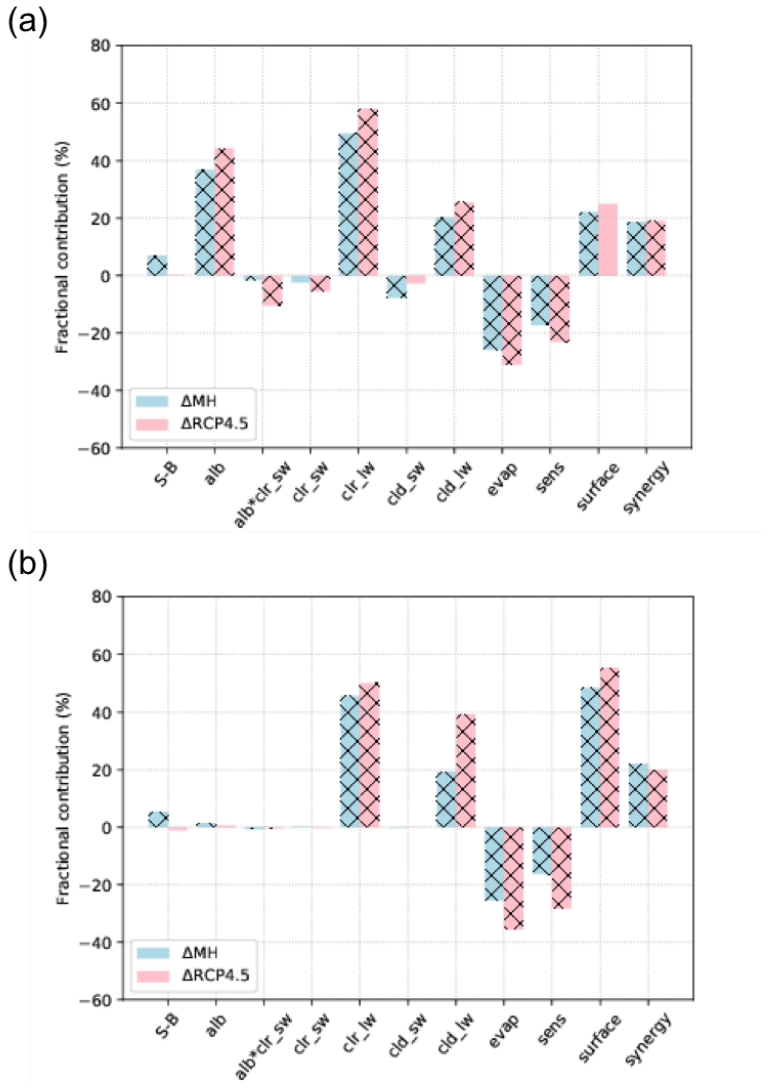

Figure 10 Fractional contribution of individual processes to the model spread in the simulated surface temperature change (%) over the ocean (north of 60°N) for ΔMH and ΔRCP4.5: (a) annual mean; and (b) October-November-December mean. The sum of the bar graphs in the same color for each plot adds up to 100%. The hatching indicates the contribution is statistically significant at the 10% level. All 10 models are used. See Table 3 for the interpretation of each component.